

Numerical Analysis of the Chemical Reactions Effects on NO_x Conversion under Various Reduced Electric Fields

Nedjwa Djaouani^{1*}, Mostefa Lemerini¹ and Omar Sabbar Dahham²

¹Department of Physics, Faculty of Sciences, University of Tlemcen, Tlemcen (13000), Algeria.

²Center of Excellence Geopolymer and Green Technology, Faculty of Engineering Technology, University Malaysia Perlis, Kampus Unicity AlamSg. Chuchuh, 02100 Padang Besar (U), Perlis, Malaysia.

Received 27 October 2017; Revised 3 February 2018; Accepted 23 April 2018

ABSTRACT

The purpose of this work is to investigate the contribution of different chemical reactions that participate in NO_x creation or reduction in N₂/O₂/H₂O/CO₂ mixed gas induced by negative corona discharge under different reduced electric field levels: 100 - 200 Td (1Td=10⁻²¹ V.m²). The fundamental chemistry governing NO_x evolution developed in this paper is based on a full set of processes regrouped in 200 selected chemical reactions involving 36 molecular, excited, atomic, and charged species. The density was calculated using the continuity equation while not the diffusion term, and the time analysis varied from 10⁻⁹ to 10⁻³s. The results of simulations show the role played by different chemical reactions on NO_x conversion. It is shown that at 100 Td near 60% of NO can be removed by radical O₄⁻ through the reaction NO + O₄⁻ → NO₃⁻ + O₂ and near 20% of NO₂ and NO₃ could be removed by radicals O₃⁻ and O₂⁻ through NO₂ + O₃⁻ → NO₂⁻ + O₃ and NO₃ + O₂⁻ → NO₃⁻ + O₂ respectively.

Keywords: Plasma Chemistry; Rate Constant; No_x Conversion; Chemical Kinetic; Gas Discharge.

1. INTRODUCTION

Generally, the reduced electric field (E/N ratio) is considered a critical parameter controlling the electron energy in plasma discharges. The chemistry of plasma can be different based on the value of E/N ratio. For several years, the common catalytic and thermal methods used to eliminate or at least to reduce the level of NO_x that existed in industrial flue gas and/or generated by the vehicles will not permit us to respect the limits of gases emission, which has become more dangerous in the environment. J.L. Walsh, P. Olszewski and al [1, 2] studied the properties of Ar/O₂ microwave, driven surface on plasmas as a function of the Ar/O₂ ratio in the gas mixture. The key parameters are the plasma electron density and electron temperature, which are estimated with Thomson scattering (TS) for O₂ contents up to 50% of the total gas flow. N C Roy and al [3] used an optical emission spectroscopic (OES) diagnostic technique for the characterization of plasmas and for identifications of OH and O radicals along with other species in the plasmas. Walsh et al [4, 5] showed in experimental studies at atmospheric pressure plasma jets in helium that, for jets extending beyond the guiding tube, the propagation can be temporarily halted by neutralizing the applied voltage by applying the same voltage to two external electrodes surrounding the jet. Chang J S et al have investigated the influences on the applications such as electron beam processing. It has been predominantly studied for treatment of gaseous effluents polluted by NO_x [6-7] and/or ozone production [8-11], medical applications [12-16] and surface treatment [17-18]. Therefore, new more effective depolluting methods are at present studied and the use of non-thermal plasmas made by electrical discharge or electron beam

*Corresponding author: n.djaouani@yahoo.com

processing [19–25] seem suitable techniques. The energetic electrons generated by the electrical discharge collide with the background gas molecules, thus creating long-lived molecular and atomic free radicals that interact with the pollutants and convert them, during the post-discharge, into clean or easy to collect yields through a complex set of chemical and physical reactions.

Several researchers have previously studied the influences of non-equilibrium discharges gas dynamics at atmospheric pressure [26–29]. These influence can be thermal (correlated movements) or dynamic (collective movement of drift) by nature. The charged particles, specifically the ions, can transfer a part of their derivative movement to the neutral ones. The fluid motion induced by an electric discharge is indicated to as an ion wind or electric wind. This case was proved before and extensively studied in the case of the corona discharge between the plane and the tip [29-31]. The charged particles generated in the inter electrode space are usually accelerated by the electric field E . It is known that the electrical proprieties depend on the reduced field E/N , where E is the electric field and N is the neutral gas density [32-34], and raise the internal energy of the neutral gas. During the post-discharge phase, the vibrational energy reservoir slowly relaxes resulting light warming of the ionized channel and a local decrease in the density of the gas. The chemical reactivity of the neutral gas mixture allows the toxic molecule transformation into harmless particles (such as N or N_2O) or to generate acids (such as HNO_3) inside the plasma. This type of acid can be converted into salt (by addition of a base) [35-38].

Herein, the aim of the current work is to simulate numerically, under various reduced electric field (100 -200 Td) values, the time evolution of 36 chemical species such as atoms (H, O and N), molecules ($O_2, N_2, CO_2, OH, H_2O, HO_2, HNO_3, O_3, CO$, and H_2), nitric oxides (NO, NO_2, NO_3, N_2O and N_2O_5), negative ions ($NO_2^-, NO_3^-, O^-, O_2^-, O_3^-$ and O_4^-), positive ions ($O^+, N^+, NO^+, N_2^+, O_2^+$ and O_4^+), excited species ($O_2(a_1\Delta_g), N_2(A^3\Sigma_u^+), O(^1D), N(^2D), N(^2P)$) and electrons (e) in the mixture (N_2 : 76%, O_2 : 12%, CO_2 : 6%, and H_2O : 6%). These different species react following 200 selected chemical reactions. In this numerical simulation, we presume numerous effects induced by the corona discharge passage in a mixed gas. In order to simplify this study, we suppose that the gas has no convective movement gradients and the pressure remains constant.

2. MATHEMATICAL MODEL

The mathematical model applied in this study comprises a system of equations, which takes into consideration the density variation and the chemical kinetics of the environment. A numerical code of zero order was developed to resolve the transport equations for charged and neutral particles. The algorithm is based on the time integration of the equations system under consideration the density variation and the chemical kinetics of the environment. The equation systems of chemical kinetics can be described by an ordinary differential equation system, as shown below:

$$\frac{dN_i}{dt} = \sum_{j=1}^{j_{\max}} Q_{ij} \quad \text{where } j = 1, \dots, j_{\max} \quad (1)$$

$$Q_{ij} = (G_{ij} - L_{ij}) \quad (2)$$

Where N_i is the species densities vector, $i=1$ up to 36 considered in the plasma and Q_{ij} the source term vector depending on the reaction coefficients and corresponding to the contributions from different processes. G_{ij} and L_{ij} is the gain and loss of species i during the chemical reactions $j=1$ up to $j_{\max}=200$. The solution of such a system requires the knowledge of the initial concentrations. The total density N of the gas is given by the ideal gas law:

$$P = Nk_b T \quad (3)$$

Where P is the pressure, k_b Boltzmann constant and T is the absolute temperature. The gas reactivity is taken into consideration in the source term Q_{ij} of the density conservation Eq. (1).

$$G_{ij} = \sum_{\alpha} K_{\alpha}(T)(n_i n_j)_{\alpha} \quad (4)$$

$$L_{ij} = \sum_{\beta} K_{\beta}(T)(n_i n_j)_{\beta} \quad (5)$$

$K_{\alpha}(T)$ and $K_{\beta}(T)$ are the coefficients of the chemical reaction number α or β and $(n_i n_j)$ is the product of densities of species i and j interacting in response to the reaction α or β . These coefficients satisfy Arrhenius formula:

$$K_{\alpha}(T) = A. \exp\left(\frac{-\theta_{\alpha}}{T}\right) \quad (6)$$

$$K_{\beta}(T) = B. \exp\left(\frac{-\theta_{\beta}}{T}\right) \quad (7)$$

Where A and B are the constants factor and θ_{α} and θ_{β} are the activation energy of the reaction and T the absolute temperature of the species involved in the warm rain that has left the chemical reaction.

Table 1. Main reactions contributing to generation and destruction of NO_x and their rate constants. (The units of rate constants are in $cm^3 \cdot molecule^{-1} \cdot s^{-1}$ for two body reactions, whereas $cm^6 \cdot molecule^{-2} \cdot s^{-1}$ for three body reactions).

	Reactions	Rate constants	Ref.
R1	$e + O_2 \rightarrow O + O + e$	$k_1 = 15 \times 10^{-9}$	[32]
R2	$e + N_2 \rightarrow N + N + e$	$k_2 = 2.05 \times 10^{-11}$	[32]
R3	$e + H_2O \rightarrow OH + H + e$	$k_3 = 3.35 \times 10^{-10}$	[32]
R4	$e + CO_2 \rightarrow CO + O + e$	$k_4 = 8.7 \times 10^{-11}$	[27]
R5	$N(^2D) + O_2 \rightarrow NO + O$	$k_5 = 5.2 \times 10^{-12}$	[34]
R6	$N + O_3^- \rightarrow NO + O_2 + e$	$k_6 = 5.0 \times 10^{-10}$	[27]
R7	$O + NO_3^- \rightarrow NO + O_3 + e$	$k_7 = 1.5 \times 10^{-10}$	[27]
R8	$NO + O_4^- \rightarrow NO_3^- + O_2$	$k_8 = 2.5 \times 10^{-10}$	[34]
R9	$NO + O_3^- \rightarrow NO_3^- + O$	$k_9 = 1.0 \times 10^{-11}$	[34]
R10	$NO + O_3^- \rightarrow NO_2^- + O_2$	$k_{10} = 2.6 \times 10^{-12}$	[34]
R11	$H + NO_2 \rightarrow NO + OH$	$k_{11} = 1.15 \times 10^{-10}$	[32]
R12	$NO + HO_2 \rightarrow NO_2 + OH$	$K_{12} = 1.1 \times 10^{-11}$	[27]
R13	$N + NO_3^- \rightarrow NO_2 + NO + e$	$K_{13} = 5.0 \times 10^{-10}$	[27]
R14	$NO_2^- + N_2O_5 \rightarrow 2NO_2 + NO_3^-$	$k_{14} = 7.0 \times 10^{-10}$	[32]
R15	$N + O_2^- \rightarrow NO_2 + e$	$k_{15} = 5.0 \times 10^{-10}$	[34]
R16	$NO_2 + O_3^- \rightarrow NO_2^- + O_3$	$k_{16} = 7.0 \times 10^{-11}$	[34]
R17	$NO_2 + O_3^- \rightarrow NO_3^- + O_2$	$k_{17} = 2.0 \times 10^{-11}$	[34]
R18	$NO_2 + O_2^- \rightarrow NO_2^- + O_2$	$k_{18} = 7.0 \times 10^{-10}$	[34]
R19	$NO_3^- + O_4^+ \rightarrow NO_3 + O_2 + O_2$	$k_{19} = 1.0 \times 10^{-7}$	[27]
R20	$NO_3^- + NO^+ \rightarrow NO_3 + N + O$	$k_{20} = 1.0 \times 10^{-7}$	[34]
R21	$OH + HNO_3 \rightarrow NO_3 + H_2O$	$k_{21} = 1.3 \times 10^{-13}$	[27]
R22	$NO_3 + O_2^- \rightarrow NO_3^- + O_2$	$k_{22} = 5. \times 10^{-10}$	[27]
R23	$NO_3 + OH \rightarrow NO_2 + HO_2$	$k_{23} = 2.6 \times 10^{-11}$	[27]
R24	$NO_3 + NO_2^- \rightarrow NO_2 + NO_3^-$	$k_{24} = 5.0 \times 10^{-10}$	[27]
R25	$H_2O + O(^1D) \rightarrow 2OH$	$k_{25} = 2.3 \times 10^{-10}$	[27]
R26	$H + O_3 \rightarrow OH + O_2$	$k_{26} = 2.8 \times 10^{-11}$	[27]
R27	$H + O^- \rightarrow OH + e$	$k_{27} = 6.5 \times 10^{-10}$	[27]

R28	$\text{HO}_2 + \text{O}_3 \rightarrow \text{OH} + 2\text{O}_2$	$k_{28} = 2.0 \times 10^{-15}$	[27]
R29	$\text{OH} + \text{O}_3 \rightarrow \text{HO}_2 + \text{O}_2$	$k_{29} = 6.5 \times 10^{-14}$	[27]
R30	$\text{OH} + \text{NO}_2 \rightarrow \text{HNO}_3$	$k_{30} = 3.5 \times 10^{-11}$	[27]
R31	$\text{OH} + \text{HO}_2 \rightarrow \text{H}_2\text{O} + \text{O}_2$	$k_{31} = 1.1 \times 10^{-10}$	[35]
R32	$\text{OH} + \text{NO}_2 + \text{O}_2 \rightarrow \text{HNO}_3 + \text{O}_2$	$k_{32} = 2.2 \times 10^{-30}$	[32]

3. RESULTS AND DISCUSSIONS

The chemical kinetics includes 36 different types of chemical species: atoms (H, O and N), molecules (O_2 , N_2 , CO_2 , OH, H_2O , HO_2 , HNO_3 , O_3 , CO, and H_2), nitric oxides (NO, NO_2 , NO_3 , N_2O and N_2O_5), negative ions (NO_2^- , NO_3^- , O^- , O_2^- , O_3^- and O_4^-), positive ions (O^+ , N^+ , NO^+ , N_2^+ , O_2^+ and O_4^+), excited species ($\text{O}_2(\text{a}_1\Delta_g)$, $\text{N}_2(\text{A}^3\Sigma_u^+)$, $\text{O}(^1\text{D})$, $\text{N}(^2\text{D})$, $\text{N}(^2\text{P})$) and electrons (e). These species react following 200 selected chemical reactions; the main ones are shown in Table 1. In this part, we will evaluate the influence of reactions rate on conversion NO_x species, we calculate in particular the reactions rate of R5 to R24 between 10^{-9} s and 10^{-3} s. These reactions in this work are the main reactions which they participate in evolution of NO, NO_2 and NO_3 species. We recall that for each species, the first three reactions contribute to the creation of the species and the other three to the destruction of the same species. For example, for nitrogen monoxide, R5, R6 and R7 reactions are involved in the production of NO whereas R8, R9 and R10 reactions are involved in the consumption of the same species.

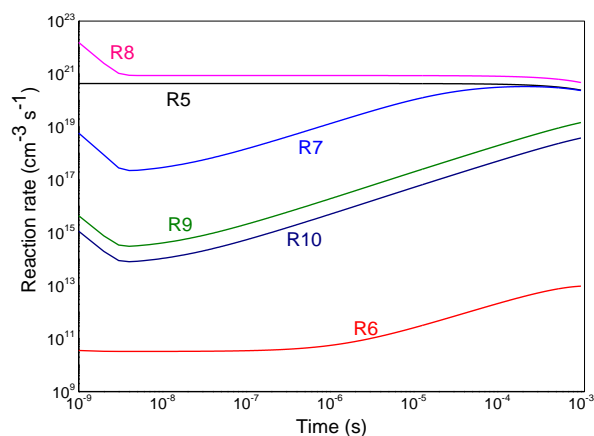


Figure 1. Time evolution of reaction rate of the main reactions that participate in the conversion of NO specie in the mixture $\text{N}_2/\text{O}_2/\text{H}_2\text{O}/\text{CO}_2$ at 100Td. The numbers are associated with the following reactions: R5: $\text{N}(^2\text{D}) + \text{O}_2 \rightarrow \text{NO} + \text{O}$; R6: $\text{N} + \text{O}_3 \rightarrow \text{NO} + \text{O}_2 + \text{e}$; R7: $\text{O} + \text{NO}_3 \rightarrow \text{NO} + \text{O}_3 + \text{e}$; R8: $\text{NO} + \text{O}_4 \rightarrow \text{NO}_3^- + \text{O}_2$; R9: $\text{NO} + \text{O}_3^- \rightarrow \text{NO}_3^- + \text{O}$; R10: $\text{NO} + \text{O}_3^- \rightarrow \text{NO}_2^- + \text{O}_2$.

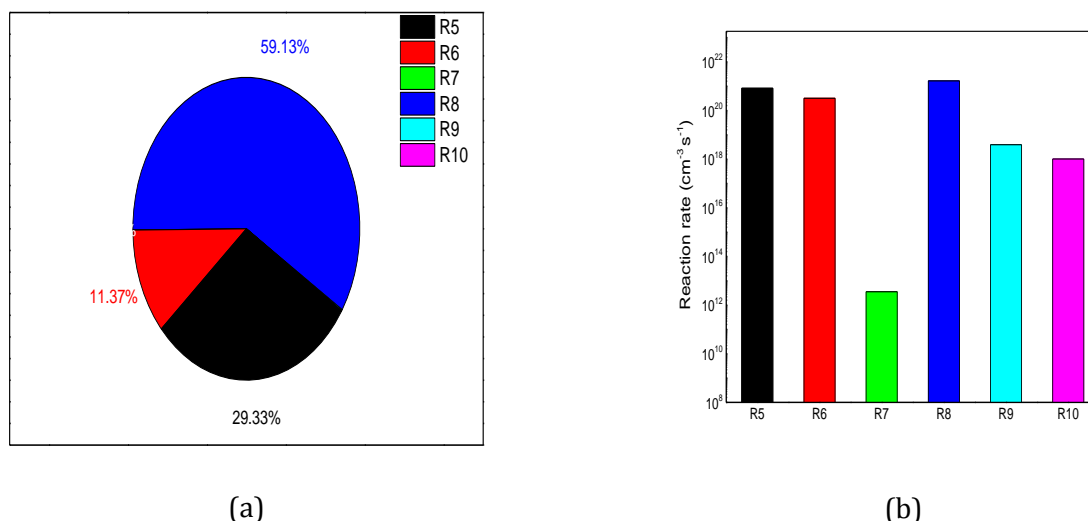


Figure 2.Representation of the main reactions (R5, R6, R7, R8, R9 and R10) contributing to the conversion of NO specie in the mixture $N_2/O_2/H_2O/CO_2$ at 100Td. (a) with percentage of different reactions; (b) with diagram of different reactions rate.

Figure 1 shows the time evolution of the main reactions contributing to NO conversion at 100 Td. As illustrated in this figure many reactions participate to the generation and destruction of NO. However, NO is generated through R5, R6 and R7 reactions:



and reduced through R8, R9 and R10 reactions:



The effects of these reactions have been represented in figure 2a with percentage and 2b with diagram of different reactions rate. Observed on this figure is the domination of $N(^2D)$ on others radicals for creation, at 29.33%, whereas for the reduction it is the radical which prevails over the others since it represents 59.13%. These results are also verified on figure 2b and resembles the phenomenon of destruction dominates that of creation.

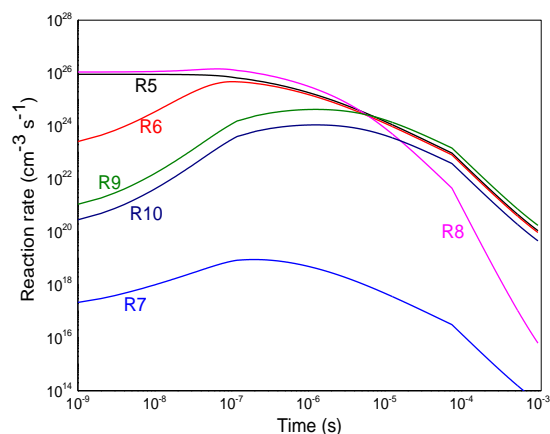


Figure 3. Time evolution of reaction rate of the main reactions that participate in the conversion of NO specie in the mixture $N_2/O_2/H_2O/CO_2$ at 200Td. The numbers are associated with the following reactions: R5: $N(^2D) + O_2 \rightarrow NO + O$; R6: $N + O_3^- \rightarrow NO + O_2 + e$; R7: $O + NO_3^- \rightarrow NO + O_3 + e$; R8: $NO + O_4^- \rightarrow NO_3^- + O_2$; R9: $NO + O_3^- \rightarrow NO_3^- + O$; R10: $NO + O_3^- \rightarrow NO_2^- + O_2$

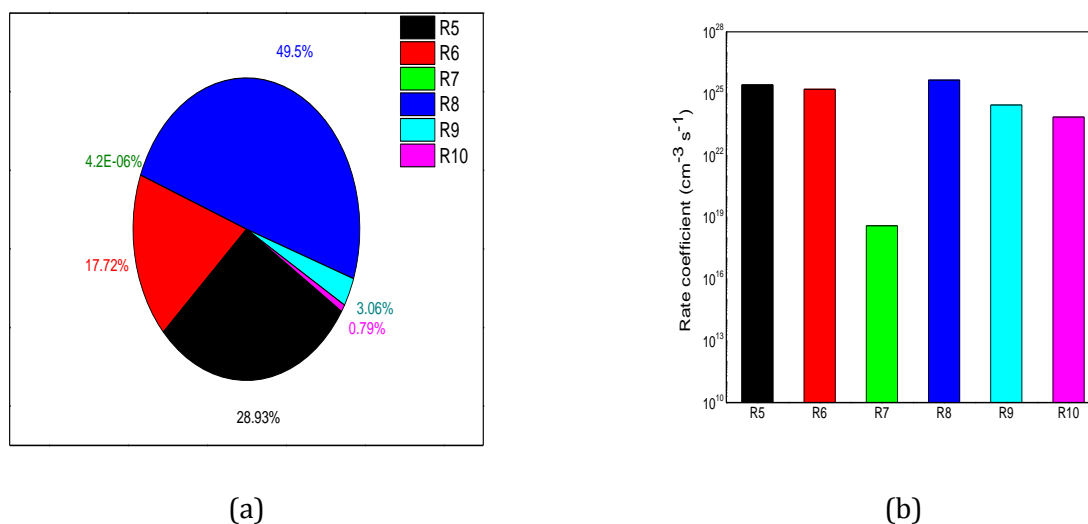


Figure 4. Representation of the main reactions (R13, R14, R15, R16, R17 and R18) contributing to NO conversion in the mixture $N_2/O_2/H_2O/CO_2$ at 200Td. (a) with percentage of different reactions; (b) with diagram of different reactions rate.

Figures.3 and 4 show the evolution of reaction rate of NO at 200 Td. We notice on all the figures that the reduction of nitrogen monoxide is always higher than that of the creation but with a smaller deviation than for 100Td. Indeed, the value is 53.35% for the reduction against 46.65% for the production. It is also noted that the reactions R9 and R10 which were negligible for 100Td begin to have an influence on the reduction of nitrogen monoxide for 200Td. It's found that the effects of the O_4^- ion is less dominant than in the case of 100 TD, this is due to the fact that the reactions R5, R6, decreased less rapidly than the reaction R8 with time.

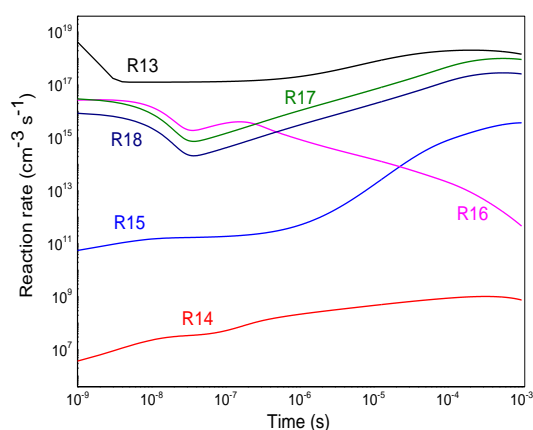
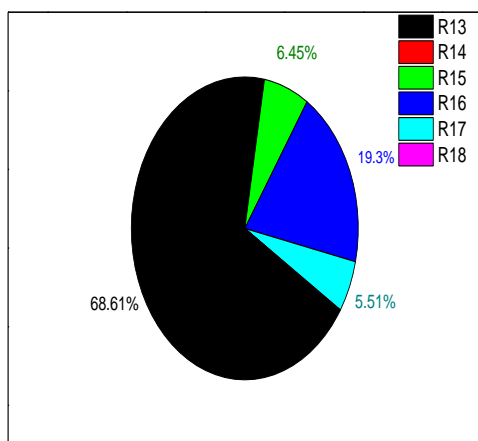
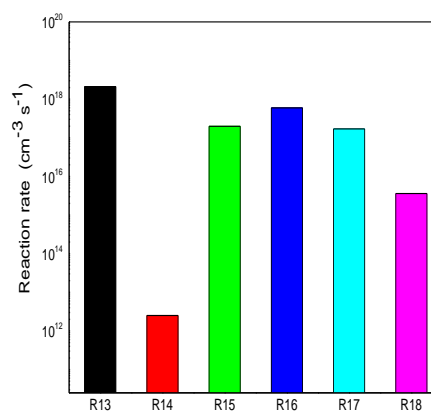


Figure 5. Time evolution of reaction rate of the main reactions that participate in the conversion of NO_2 specie in the mixture $\text{N}_2/\text{O}_2/\text{H}_2\text{O}/\text{CO}_2$ at 100Td. The numbers are associated with the following reactions: R13: $\text{N} + \text{NO}_3^- \rightarrow \text{NO}_2 + \text{NO} + \text{e}$; R14: $\text{NO}_2^- + \text{N}_2\text{O}_5 \rightarrow 2\text{NO}_2 + \text{NO}_3^-$; R15: $\text{N} + \text{O}_2^- \rightarrow \text{NO}_2 + \text{e}$; R16: $\text{NO}_2 + \text{O}_3^- \rightarrow \text{NO}_2^- + \text{O}_3$; R17: $\text{NO}_2 + \text{O}_3^- \rightarrow \text{NNO}_3^- + \text{O}_2$; R18: $\text{NO}_2 + \text{O}_2^- \rightarrow \text{NO}_2^- + \text{O}_2$.



(a)



(b)

Figure 6. Representation of the main reactions (R13, R14, R15, R16, R17 and R18) that contribute in the conversion of NO_2 specie in the mixture $\text{N}_2/\text{O}_2/\text{H}_2\text{O}/\text{CO}_2$ at 100Td. (a) with percentage of different reactions; (b) with diagram of different reactions rate.

Figure 5 shows the time evolution of the main reactions contributing to NO_2 destruction and creation at 100 Td. NO_2 is generated through R13, R14 and R15 reactions:



and reduced through R16, R17 and R18 reactions:





We continue with the same analysis as before. In general, NO_2 is formed from NO and N_2O_5 and is converted into N_2O , NO_3 and HNO_3 , while NO can be converted into NO_2 and N_2 . In our case, NO_2 is formed especially from N : 68.61% and converted into O_3 : 19.30% and O_2 : 5.51% (see Figure 6a).

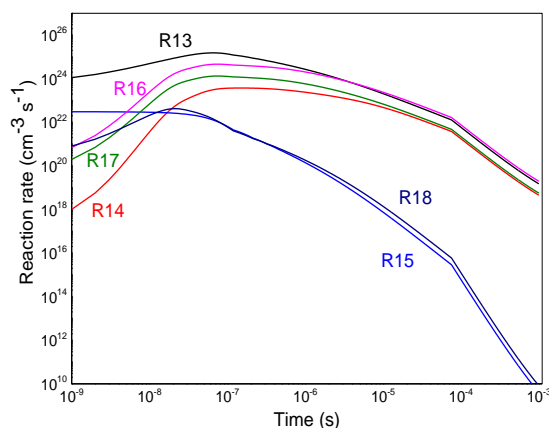


Figure 7. Time evolution of reaction rate of the main reactions that participate in the conversion of NO_2 specie in the mixture $\text{N}_2/\text{O}_2/\text{H}_2\text{O}/\text{CO}_2$ at 200Td. The numbers are associated with the following reactions: R13: $\text{N} + \text{NO}_3^- \rightarrow \text{NO}_2 + \text{NO} + e$; R14: $\text{NO}_2^- + \text{N}_2\text{O}_5 \rightarrow 2\text{NO}_2 + \text{NO}_3^-$; R15: $\text{N} + \text{O}_2^- \rightarrow \text{NO}_2 + e$; R16: $\text{NO}_2 + \text{O}_3^- \rightarrow \text{NO}_2^- + \text{O}_3$; R17: $\text{NO}_2 + \text{O}_3^- \rightarrow \text{NO}_3^- + \text{O}_2$; R18: $\text{NO}_2 + \text{O}_2^- \rightarrow \text{NO}_2^- + \text{O}_2$.

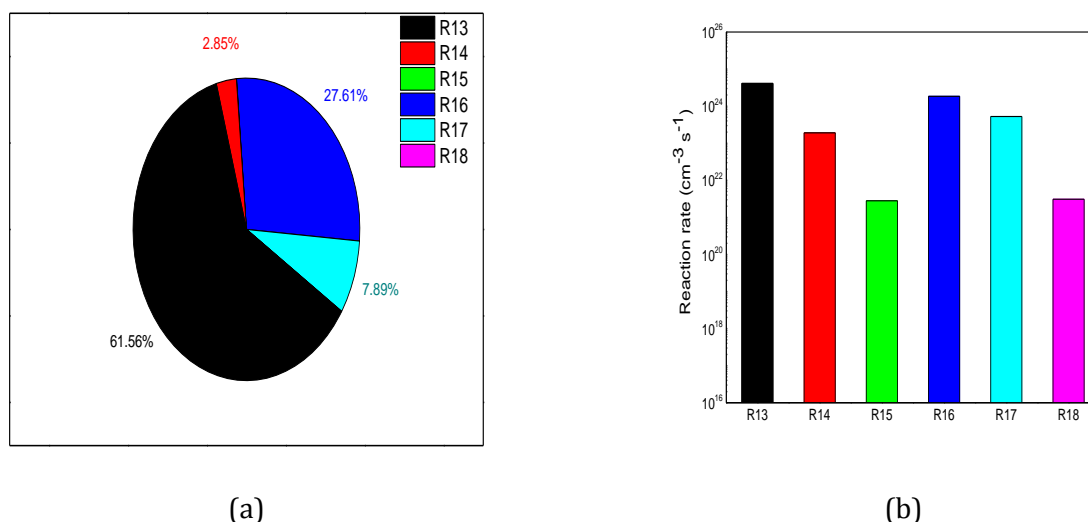


Figure 8. Representation of the main reactions (R13, R14, R15, R16, R17 and R18) that contribute in the conversion of NO_2 specie in the mixture $\text{N}_2/\text{O}_2/\text{H}_2\text{O}/\text{CO}_2$ at 200Td. (a) with percentage of different reactions; (b) with diagram of different reactions rate.

To continue the analysis, shown in Figures 7 and 8 the results for the value 200Td. We observe that the gap between production and consumption of nitrogen dioxide decreases. Indeed, we obtain 64.41% for the creation of NO_2 against 35.50% for its disappearance. It can be said that for 200Td the six reactions R13 to R18 participate in the conversion of the nitric dioxide.

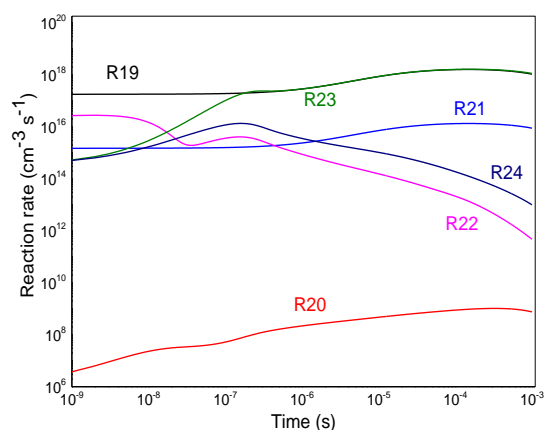


Figure 9. Time evolution of reaction rate of the main reactions that participate in the conversion of NO_3 specie in the mixture $\text{N}_2/\text{O}_2/\text{H}_2\text{O}/\text{CO}_2$ at 100Td. The numbers are associated with the following reactions: R19: $\text{NO}_3^- + \text{O}_4^- \rightarrow \text{NO}_3 + \text{O}_2 + \text{O}_2$; R20: $\text{NO}_3^- + \text{NO}^+ \rightarrow \text{NO}_3 + \text{N} + \text{O}$; R21: $\text{OH} + \text{HNO}_3 \rightarrow \text{NO}_3 + \text{H}_2\text{O}$; R22: $\text{NO}_3 + \text{O}_2^- \rightarrow \text{NO}_3^+ + \text{O}_2$; R23: $\text{NO}_3 + \text{OH} \rightarrow \text{NO}_2 + \text{HO}_2$; R24: $\text{NO}_3 + \text{NO}_2^- \rightarrow \text{NO}_2 + \text{NO}_3^-$.

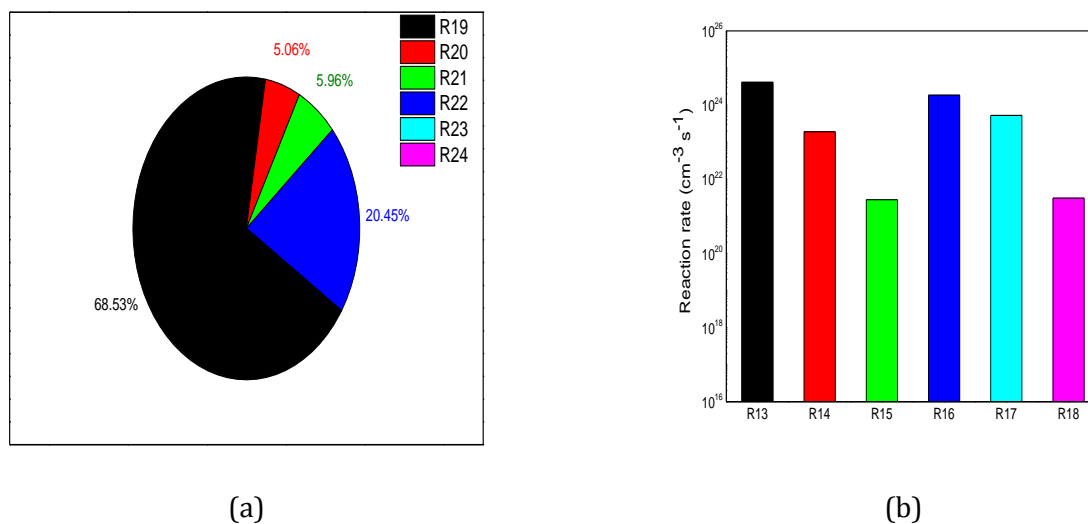


Figure 10. Representation of the main reactions (R19, R20, R21, R22, R23 and R24) that contribute in the conversion of NO_3 specie in the mixture $\text{N}_2/\text{O}_2/\text{H}_2\text{O}/\text{CO}_2$ at 100Td. (a) with percentage of different reactions; (b) with diagram of different reactions rate.

To complete our study we have shown in Figures 9 and 10 the results obtained for the specie NO_3 at 100Td. A much larger creation than that of NO_2 was observed following the participation of the three R19, R20 and R21 reactions giving a rate of 79.55% compared with 20.45% reduction for the other reactions R22, R23 and R24.

Figure 9 shows the time evolution of the main reactions contributing to NO_3 destruction and creation. NO_3 is generated through R19, R20 and R21 reactions:



And reduced through R22, R23 and R24 reactions:

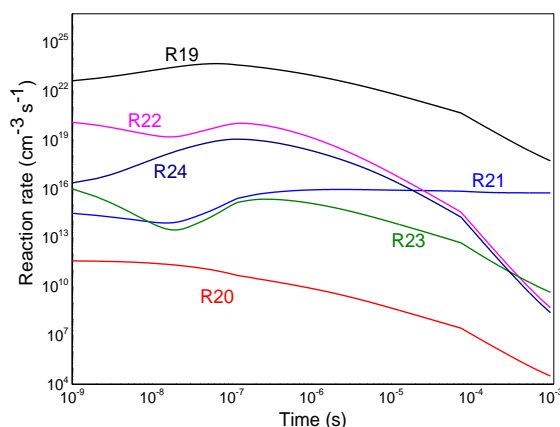


Figure 11. Time evolution of reaction rate of the main reactions that participate in the conversion of NO_3 specie in the mixture $\text{N}_2/\text{O}_2/\text{H}_2\text{O}/\text{CO}_2$ at 200Td. The numbers are associated with the following reactions: R19: $\text{NO}_3^- + \text{O}_4^+ \rightarrow \text{NO}_3 + \text{O}_2 + \text{O}_2$; R20: $\text{NO}_3^- + \text{NO}^+ \rightarrow \text{NO}_3 + \text{N} + \text{O}$; R21: $\text{OH} + \text{HNO}_3 \rightarrow \text{NO}_3 + \text{H}_2\text{O}$; R22: $\text{NO}_3 + \text{O}_2^- \rightarrow \text{NO}_3^- + \text{O}_2$; R23: $\text{NO}_3 + \text{OH} \rightarrow \text{NO}_2 + \text{HO}_2$; R24: $\text{NO}_3 + \text{NO}_2^- \rightarrow \text{NO}_2 + \text{NO}_3^-$.

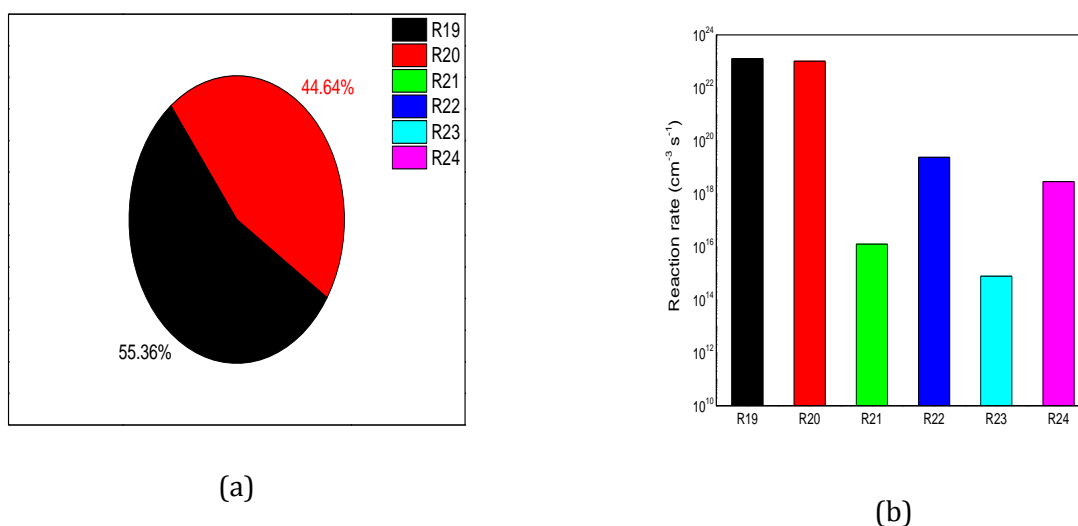


Figure 12. Representation of the main reactions (R19, R20, R21, R22, R23 and R24) that contribute in the conversion of NO_3 specie in the mixture $\text{N}_2/\text{O}_2/\text{H}_2\text{O}/\text{CO}_2$ at 200Td. (a) with percentage of different reactions; (b) with diagram of different reactions rate.

Finally, in Figure 11 and 12 we have represented the evolution of the species NO_3 for the value 200Td. We observed the dominance of the creation of this species following the evolution of the two other species previously studied, namely nitrogen monoxide NO and nitrogen dioxide NO_2 . The creation rate reaches 99.99% thanks to the reactions R19 and R20.

4. CONCLUSION

In this work, the influence of chemical reactions, which actively participate in the conversion of nitrogen oxides in the gas mixture $N_2/O_2/H_2O/CO_2$ in the range 100 - 200 Td were investigated. In particular, we wanted to know the reaction rate of these chemical reactions in this gas mixture and to specify the species that play a decisive role in the creation or destruction of nitrogen oxides. We have focused on three species that are nitrogen monoxide NO, nitrogen dioxide NO_2 and nitrogen trioxide NO_3 that are the main constituents of nitrogen oxides.

The results obtained show a strong dependence on the reduced electric field and between the species themselves. Indeed, we have noticed that the evolution of one species can influence the evolution of another specie. They can be summarized as follows.

- (i) The mechanism of NO creation occurs mainly by the reaction of N (2D) radicals with molecular oxygen:

$N(^2D) + O_2 \rightarrow NO + O$, and destruction by O_4^- radicals with: $NO + O_4^- \rightarrow NO_3^- + O_2$. We have obtained 29.33% at 100 Td against 28.93% at 200 Td for creation, and 59.13% at 100 Td against 49.50% at 200 Td for destruction.

- (ii) The mechanism of NO_2 production is due mainly to the reaction of NO_3^- radicals with atomic nitrous:

$N + NO_3^- \rightarrow NO_2 + NO + e$, and reduction by reaction: $NO_2 + O_3^- \rightarrow NO_2^- + O_3$. At 100 Td we have found 68.61% for production against 61.65% at 200 Td, and 19.30% at 100 Td against 27.61% at 200 Td for consumption.

- (iii) About NO_3 it is shown that the creation is due to two radicals O_4^+ and NO^+ through reactions:

$NO_3^- + O_4^+ \rightarrow NO_3 + 2O_2$, and $NO_3^- + NO^+ \rightarrow NO_3 + N + O$, and reduction by reaction: $NO_3 + O_2^- \rightarrow NO_3^- + O_2$.

We note that at 200 Td, there is no reduction and the two reactions participated completely to the Production of NO_3 (55.36% for R19 and 44.64% for R20). This is the effect of transformation of NO and NO_2 .

Finally, the obtained results clearly show the important role played by chemical reactions on NO_x removal and creation under reduced electric field.

REFERENCES

- [1] J. L. Walsh, P. Olszewski and J.W. Bradley, *Plasma Sources Sci. T.* **21**, 3 (2012) 034007.
- [2] S. Espinho, S. Hofmann, J. M. Palomares and S. Nijdam, " The influence of the Ar/ O_2 ratio on the electron density and electron temperature in microwave discharges " , *Plasma Sources Science and Technology* **26**, 10 (2017).
- [3] N. C. Roy, M.R. Talukder and A. N. Chowdhury, " OH and O radicals production in atmospheric pressure air/Ar/ H_2O gliding arc discharge plasma jet" , *Plasma Sources Science and Technology* **19**, 12 (2017).
- [4] J.L. Walsh and G.V. Naidis, *J. Phys. D: Appl. Phys.* **46**, 9 (2013) 095203.
- [5] J.S. Chang, *Plasma Sources Sci. Technol.* **17** (2008) 045004.
- [6] M. Laroussi, *IEEE Trans. Plasma Sci.* **24** (1996) 1188.
- [7] M. Simek and M. Clupek, *J. Phys. D: Appl. Phys.* **35** (2002) 1171.
- [8] Eliasson and U. Kogelschatz, *IEEE Trans. Plasma Sci.* **19**(1991) 1063.
- [9] J. Chen and J.H. Davidson, *Plasma Chem. Plasma Process* **22** (2002) 495.

- [10] S.Yu. Akishev, A.A. Deryugin, I.V. Kochetov, *J. Phys. D: Appl. Phys.* **26** (1993)1630.
- [11] M. Laroussi, A.Fridman, P. Favia, and M.R. Wertheimer, *Plasma Process. Polym.***7** (2010) 193.
- [12] A. M. Pointu, A. Ricard, E.Odic, M. Ganciu, *Plasma Process.Polym.***5** (2008) 559.
- [13] C. C. Wang and S. J. Roy, *Appl. Phys.***106** (2009) 013310.
- [14] E. Moreau, *J. Phys. D: Appl. Phys.***40** (2007) 605.
- [15] G. Fridman, G. Friedman, A.Gutsol, A. B. Shekhter, V.N. Vasilets, and A. Fridman, *Plasma Processes and Polymers***5**(2008) 503.
- [16] Tendero C., " Torche plasma micro-onde à la pression atmosphérique: application autraitement de surfaces métalliques Ph.D". Université de Limoges, France (2005).
- [17] L. Miao, S. Tanemura, H. Watanabe, Y. Mori, K. Kaneko and S.J. Toh, *Crystal Growth***260** (2004) 118.
- [18] F. Fresnet, G. Baravian, L. Magne, S. Pasquiers, C. Postel, V. Puech and A. Rousseau, *Plasma Sources Sci. Technol.***11** (2002) 152.
- [19] M. Baeva, A. Pott and J.Uhlenbusch, *Plasma Sources Sci. Technol.* **11**(2002) 135.
- [20] B. Eliasson and U. Kogelschatz, *IEEE Trans. Plasma Sci.* **19** (1991) 1065.
- [21] B. M. Penetrante, J. N. Bardsley, M. C. Hsiao, *Japan. J. Appl. Phys.* (36)(1997) 5007.
- [22] B. M. Penetrante and S. E. Schultheis (eds), " Non-Thermal Plasma Techniques for Pollution Control parts A and B ", Springer, Berlin (1993).
- [23] A. K. Ferouani, M. Lemerini and B.Liani, *Numerical Modelling Chap 7*, Edited by PreepMiidla Croatia,(2012) 143-156.
- [24] W. Sun, B. Pashaie, S. Dhaliand F. I. Honea, *J. Appl. Phys.* **79** (1996) 3438.
- [25] N. Spyrou, B. Held, R.Peyrous, Held, C. Manassis and P.Pignolet, *J.Phys. D: Appl. Phys.*, **25**(1992) 211.
- [26] Y. Creyghton, "Pulsed positive corona discharges: fundamental study and application to flue gas treatment Ph.D". Technische University of Eindhoven, Netherlands (1994).
- [27] J. Batina, F. Noël, S.Lachaud, R. Peyrous and J.F. Loiseau, *J. Phys. D: Appl. Phys* **34** (2001) 1510.
- [28] R. Ono and T. Oda, *Japanese Journal of Applied Physics***43** (2004) 321.
- [29] O. Eichwald, M. Yousfi, A.Hennad and M. D. Benabdessadok, *J. Appl. Phys.***82** (1997) 4781.
- [30] L. B. Loeb, " Electrical Coronas, Their basic physical mechanism Ph.D". Univ. of California Press, Berkeley and Los Angeles (1965).
- [31] J. F. Loiseau, J. Batina, F. Noël, and R. Peyrous, *J. Phys. D: Appl. Phys.* **35** (2002) 1020.
- [32] L. Zhao, K. Adamiak, *Journal of Electrostatics***63**(2005) 337.
- [33] A. Flitti and S. Pancheshnyi, *Eur. Phys.J. Appl. Phys.* **45** (2009) 21001.
- [34] H. Kim, *Plasma Process. Polym.* **1**(2004) 91-110.
- [35] S. Katsuki, K. Tanaka, T. T. Fudamoto, *Japanese Journal of Applied Physics* **45** (2006) 239.
- [36] I. A. Kossyi, A. Y. Kostinsky, A. A. Matveyev and V.P. Silakov, *Plasma Sources Sci. Technol*, **1** (1992) 207.
- [37] R. Atkinson, D. L. Baulch, R. A. Coa, R. F. Hampson Jr., J. A. Kerr and J. Troe, *J. Phys. Chem. Ref. Data* **26** (1997) 521.
- [38] Nagaraja S, Yangand V and Adamovich I., *J. Phys. D: Appl. Phys.***46**(2013) 155205.